CERN-TH/2001-215
hep-ph/0108069

arXiv:hep-ph/0108069v1 7 Aug 2001

Multijet matrix elements and shower evolution in hadronic collisions: $Wb\bar{b} + n$ jets as a case study. [1, 2]

Michelangelo L. MANGANO[(a)] **Mauro MORETTI**[(b)] **and Roberto PITTAU**[(c)]

[(a)] CERN, Theoretical Physics Division, CH 1211 Geneva 23, Switzerland
[(b)] Dipartimento di Fisica, Università di Ferrara, and INFN, Ferrara, Italy
[(c)] Dipartimento di Fisica, Università di Torino, and INFN, Turin, Italy

Abstract

We study in this paper the production, in hadronic collisions, of final states with W gauge bosons, heavy quark pairs and n extra jets (with n up to 4). The complete partonic tree-level QCD matrix elements are evaluated using the ALPHA algorithm, and the events generated at the parton level are then evolved through the QCD shower and eventually hadronised using the coherent shower evolution provided by the HERWIG Monte Carlo. We discuss the details of our Monte Carlo implementation, and present results of phenomenological interest for the Tevatron Collider and for the LHC. We also comment on the impact of our calculation on the backgrounds to $W(H \to b\bar{b})$ production, when only one b jet is tagged.

CERN-TH/2001-215
February 1, 2008

[1] Presented at the FNAL Workshop on Monte-Carlos for Run 2, April 2001, Batavia, IL.

[2] This work was supported in part by the EU Fourth Framework Programme "Training and Mobility of Researchers", Network "Quantum Chromodynamics and the Deep Structure of Elementary Particles", contract FMRX–CT98–0194 (DG 12 – MIHT).

1 Introduction

Multijet final states are characteristic of a large class of important phenomena present in high-energy collisions. QCD interactions generate multijet final states via radiative processes at high orders of perturbation theory. Heavy particles in the Standard Model (SM), such as W and Z bosons or the top quark, t, decay to multiquark configurations (eventually leading to jets) via electroweak (EW) interactions. In addition to the above SM sources, particles possibly present in theories beyond the SM (BSM) are expected to decay to multiparton final states, and therefore to lead to multijets. Typical examples are the cascade decays to quarks and gluons of supersymmetric strongly interacting particles, such as squarks and gluinos.

Whether our interest is in accurate measurements of top quarks or in the search for more exotic states, multijet final states always provide an important observable, and the study of the backgrounds due to QCD is an essential part of any experimental analysis.

In addition to fully hadronic multijet final states, a special interest exists in final states where the jets are accompanied by gauge bosons. For example, the associated production of several jets with a Z boson decaying to neutrinos gives rise to multijet+missing transverse energy ($\not\!\!E_T$) final states. These provide an important background to the search for supersymmetric particles. Likewise, the associated production of 4 jets and a W boson decaying leptonically provides the leading source of backgrounds to the identification and study of top quark pairs in hadronic collisions.

Several examples of calculation of multijet cross-sections in hadronic collisions exist in the literature. Some of them are included in parton-level Monte Carlo (MC) event generators, where final states consisting of hard and well isolated partons are generated. Among the most used and best documented examples are PAPAGENO [1] (a compilation of several partonic processes), VECBOS [2] (for production of W/Z bosons in association with up to 4 jets), NJETS [3] (for production of up to 6 jets). In addition to these ready-to-use codes, programs for the automatic generation of user-specified parton-level processes exist, and have been used for the calculation of many important processes in hadronic collisions: MADGRAPH [4], CompHEP [5] and GRACE [6].

Studies of the partonic final states can be performed by assuming that each hard parton can be identified with a jet, and that the jets' momenta are equal to those of the parent parton. This simplification is extremely useful to get rough estimates of production rates, but cannot be used in the context of realistic detector simulations, for which a representation of the full structure of the final state (in terms of hadrons) is required. This full description can be obtained by merging the partonic final states with so-called shower MC programs (such as HERWIG [7], PYTHIA [8] or ISAJET [9]), where partons are perturbatively evolved through emission of gluons, and subsequently hadronized. As we shall discuss in the following, however, this merging is not always possible, since common parton-level MC's sum and average over flavours and colours, and do not usually provide sufficient information on the flavour and colour content of the events.

The goal of the present work is twofold. First we review a general strategy proposed in [10] for the construction of event generators for multijet final states, based on the exact leading-order (LO) evaluation of the matrix elements for assigned flavour and colour configurations, and the subsequent

shower development and transition into a fully hadronized final state. In view of the complexity of the problem, we shall argue in favour of the use of the algorithm ALPHA [11] as the best possible tool to carry out the relative matrix-element computations. Applications of ALPHA to the case of hadronic collisions have already been shown successful in the case of multijet production in [12, 10].

Then we apply the technique to the specific example of production of $WQ\bar{Q} + n$-jet final states (with Q being a massive quark, and $n \leq 4$). The matrix-element calculation and the generation of parton-level events is completed with the shower evolution and hadronization generated by the HERWIG MC [7]. We present the results, in the case of $Q = b$, of the parton-level calculations for several production rates and distributions of interest at the Tevatron and at the LHC. We discuss some interesting features of the final states, exploring in particular the relative size of processes where the b and $\bar{b}$ give rise to either 1 or 2 taggable jets. This comparison will underscore the importance of full matrix-element calculations taking fully into account the heavy-quark mass effects. We then present some results relative to final states reconstructed after the shower evolution. We compare parton-level to jet-level distributions, and study the ability of HERWIG to approximate the emission rate of extra jets via the shower evolution. Independent work on the merging of parton-level calculations with shower MC's (for the specific case of PYTHIA) has been pursued by the CompHEP group [13] and by the GRACE group [14], limited however to final states with at most 4 partons.

We conclude this presentation by listing future projects which could be realized within the framework of the approach presented here.

2 Matrix-element evaluation

The emission of soft gluon radiation in state-of-the-art shower-evolution programs accounts for quantum coherence, which is implemented via the prescription of angular ordering in the parton cascade [15]. Angular ordering dictates that the radiation emitted by a colour dipole be confined within the cone defined by the directions of the two colour charges defining the dipole itself. The set of colour connections among the partons which defines the set of dipoles for a given event will be called a *colour flow*, or *colour configuration*.

The comparison with existing hadron-collider data [16], confirms that the constraint of angular ordering is essential to properly describe the particle multiplicity and the momentum distribution inside jets, as well as to describe the correlations between primary jets and softer jets emitted during the shower evolution. In order to reliably evolve a multiparton state into a multijet configuration, it is therefore necessary to associate a specific colour-flow pattern to each generated parton-level event. This requires an ad-hoc approach to the evaluation of the matrix elements. A specific proposal was presented in [10], and will be shortly summarized here.

2.1 Reconstruction of colour flows

We discuss for simplicity the case of multigluon processes [17], as the extensions to cases with quarks and electroweak particles [18, 19] follow the same pattern. The scattering amplitude for n

gluons with momenta p_i^μ, helicities ϵ_i^μ and colours a_i (with $i = 1, \ldots, n$), can be written as [17]:

$$M(\{p_i\},\{\epsilon_i\},\{a_i\}) \;=\; \sum_{P(2,3,\ldots,n)} \mathrm{tr}(\lambda^{a_{i_1}}\,\lambda^{a_{i_2}}\ldots\lambda^{a_{i_n}})\; A(\{p_{i_1}\},\{\epsilon_{i_1}\};\ldots\{p_{i_n}\},\{\epsilon_{i_n}\})\;. \qquad (1)$$

The sum extends over all permutations P_i of $(2, 3, \ldots, n)$, and the functions $A(\{P_i\})$ (known as *dual* or *colour-ordered* amplitudes) are gauge-invariant, cyclically-symmetric functions of the gluons' momenta and helicities. Each dual amplitude $A(\{P_i\})$ corresponds to a set of diagrams where colour flows from one gluon to the next, according to the ordering specified by the permutation of indices. When summing over colours the amplitude squared, different orderings of dual amplitudes are orthogonal at the leading order in $1/N^2$:

$$\sum_{\mathrm{col's}} |M(\{p_i\},\{\epsilon_i\},\{a_i\})|^2 \;=\; N^{n-2}(N^2-1)\sum_{P_i}\left[|A(\{P_i\})|^2 + \frac{1}{N^2}(\mathrm{interf.})\right]. \qquad (2)$$

At the leading order in $1/N^2$, therefore, the square of each dual amplitude is proportional to the relative probability of the corresponding colour flow. Each flow defines, in a gauge invariant way, the set of colour currents which are necessary and sufficient to implement the colour ordering prescription necessary for the coherent evolution of the gluon shower. Because of the incoherence of different colour flows, each event can be assigned a specific colour configuration by comparing the relative size of $|A(\{P_i\})|^2$ for all possible flows.

When working at the physical value of $N_c = 3$, the interferences among different flows cannot be neglected in the evaluation of the square of the matrix element, eq. (1). As a result, the basis of colour flows does not provide an orthogonal set of colour states, and a MC selection of colour flows is not possible. In [10] we proposed to use the Gell-Mann basis of $SU(3)$ matrices as an orthogonal basis to represent the colour state of a given set of partons:

$$\lambda^1 = \frac{1}{\sqrt{2}}\begin{pmatrix}0&1&0\\0&0&0\\0&0&0\end{pmatrix} \quad,\quad \lambda^2 = \frac{1}{\sqrt{2}}\begin{pmatrix}0&0&1\\0&0&0\\0&0&0\end{pmatrix} \quad,\quad \lambda^3 = \frac{1}{\sqrt{2}}\begin{pmatrix}0&0&0\\1&0&0\\0&0&0\end{pmatrix}$$

$$\lambda^5 = \frac{1}{\sqrt{2}}\begin{pmatrix}0&0&0\\0&0&1\\0&0&0\end{pmatrix} \quad,\quad \lambda^6 = \frac{1}{\sqrt{2}}\begin{pmatrix}0&0&0\\0&0&0\\1&0&0\end{pmatrix} \quad,\quad \lambda^7 = \frac{1}{\sqrt{2}}\begin{pmatrix}0&0&0\\0&0&0\\0&1&0\end{pmatrix}$$

$$\lambda^4 = \frac{1}{2}\begin{pmatrix}1&0&0\\0&-1&0\\0&0&0\end{pmatrix} \quad,\quad \lambda^8 = \frac{1}{\sqrt{12}}\begin{pmatrix}1&0&0\\0&1&0\\0&0&-2\end{pmatrix}$$

In this basis, only a fraction of all possible 8^n colour assignments gives rise to a non-zero amplitude. For each event, we randomly select a non-vanishing colour state for the external gluons, and evaluate the amplitude M. We then list all dual amplitudes contributing to the chosen colour configuration according to eq. (1) and, among these dual amplitudes, we randomly select a colour flow on the basis of their relative weight. In a 6-gluon amplitude, for example, a possible non-zero colour assignment is given by $(2, 7, 5, 6, 1, 3)$. Up to cyclic permutations, only three orderings of the colour indices give rise to non-vanishing traces: $\mathrm{tr}(\lambda^2\,\lambda^7\,\lambda^5\,\lambda^6\,\lambda^1\,\lambda^3)$, $\mathrm{tr}(\lambda^2\,\lambda^6\,\lambda^1\,\lambda^5\,\lambda^7\,\lambda^3)$ and $\mathrm{tr}(\lambda^2\,\lambda^7\,\lambda^3\,\lambda^1\,\lambda^5\,\lambda^6)$. Therefore only three dual amplitudes contribute to the full amplitude: $A(2, 7, 5, 6, 1, 3)$, $A(2, 6, 1, 5, 7, 3)$ and $A(2, 7, 3, 1, 5, 6)$. The colour ordering to be specified for

the coherent parton-shower evolution can be selected by comparing the size of the squares of $\mathrm{tr}(\lambda^2\,\lambda^{i_2}\ldots\lambda^{i_6})\,A(2,i_2,\ldots,i_6)$ for the three contributing permutations $(i_2,\ldots,i_6)$ of the colour indices.

In the limit of a large number of generated events, and in the case of processes with only gluons or with gluons and one quark-antiquark pair, this algorithm is equivalent to the colour-flow extraction algorithm proposed in [20] and employed in HERWIG. There, the full sum over all colours is performed for each event. For each event one then calculates the individual subamplitudes $M(f)$ corresponding to all possible colour flows f. The event is then assigned the colour flow $\bar{f}$ with a probability:

$$P(\bar{f}) = \frac{|M(\bar{f})|^2}{\sum_f |M(f)|^2}\ . \tag{3}$$

In the case of two or more $q\bar{q}$ pairs our prescription and that of [20] differ at order $1/N_c^2$, since by generating colour states we produce configurations whose matrix element has no leading colour contribution. One such example is the process $q_i\bar{q}_i \to q_j\bar{q}_j$, where $i,j = 1,\ldots,N_c$ are fixed colours. This transition is mediated by the gluons corresponding to the diagonal Gell-Mann matrices. The colour coefficient is trivially given by

$$\sum_a \lambda^a_{ik}\lambda^a_{jl} = \frac{1}{2}\left(\delta_{il}\delta_{jk} - \frac{1}{N_c}\delta_{ik}\delta_{jl}\right)\ , \tag{4}$$

which, when $k = i$ and $l = j$ as in the proposed example, is of order $1/N_c$. The corresponding colour flow links the quark and antiquark of the initial state, and those of the final state. No such colour flows can appear in the algorithm by Odagiri, where only colour configurations of leading order in N_c are generated.

Since the colour-flow information is only relevant for events which will be evolved through a shower MC, and since one usually does this only for unweighted events, it is sufficient to evaluate the possibly large set of dual amplitudes corresponding to a given colour state only for the small set of unweighted events. The extraction of a colour flow, therefore, does not increase significantly the computing time necessary to generate unweighted events. The full sum over colours is obtained by averaging over a large sample of events. The cross section thus obtained is correct to all orders in $1/N_c$. Relative to the prescription of [20], this approach has the advantage that the random selection of colours can in principle be optimized by exploiting the strong colour-dependence of the matrix elements (see an example along these lines in [21]).

While the algorithm proposed above can in principle be adopted in the context of any of the existing calculational techniques, including those based on the automatic generation of matrix-elements such as CompHEP, MADGRAPH or GRACE, the flexibility to calculate amplitudes relative to fixed colour states, as well as those relative to dual amplitudes, and the ability to efficiently calculate matrix elements for processes with large numbers of final-state partons, single out in our view the ALPHA algorithm as the best suitable tool. The ability to tackle computations of this complexity in the case of hadronic collisions was proved in [10, 12].

3 $\mathbf{W}Q\overline{Q} + n$ jets production

The associated production of W bosons and heavy quarks ($Q = b, t$) is one of the most important background processes to several searches for new physics, as well as to the detection of top quarks. The final state $Wb\bar{b}$ is also the leading irreducible background to the production of SM Higgs bosons via the process $p\overset{(-)}{p} \to W(H \to b\bar{b})$. The relative matrix elements have been known for long time [22]. The NLO corrections to the final states where both b and $\bar{b}$ are hard and can be treated as massless have recently become available [23]. The process $p\overset{(-)}{p} \to Wb\bar{b}j$ has been studied for massive b at LO in [24], while the processes with up to two extra jets, but again in the limit of massless b, are included in VECBOS [2].

The extension to larger jet multiplicities, and the inclusion of mass effects, are necessary, among other things, to allow more accurate studies of the backgrounds to $t\bar{t}$ production. In this case, final states have typically 2 jets in addition to the $b\bar{b}$ pair, but initial and final state radiation can lead to the presence of extra jets. As we shall show later, the increase in the number of light jets in the final state which the background calculation should be able to cope with is also mandated by the need to account for background configurations where only one jet can be reconstructed from the $b\bar{b}$ system.

As an application of our techniques, we then carried out the calculation of the process $p\overset{(-)}{p} \to (W \to \ell\nu_\ell) + Q\overline{Q} + n$-jets, covering final states with up to $n = 4$ jets in addition to the heavy-quark pair. The full spin correlations between the leptons from the W decay and the other particles are included in the matrix element, as well as the finite width of the W, described by a Breit-Wigner. For simplicity, in the following we shall however always refer to the W, instead of the lepton pair which is used in the actual computations.

The classes of processes necessary to describe these final states, and with up to 2 light-quark pairs, are listed here:

$$PROC = 1: \quad q\bar{q}' \to Wb\bar{b} \tag{5}$$

$$PROC = 2: \quad qg \to Wb\bar{b}\bar{q}' \tag{6}$$

$$PROC = 3: \quad gg \to Wb\bar{b}q\bar{q}' \tag{7}$$

$$PROC = 4: \quad (q\bar{q}' \to Wb\bar{b}q''\bar{q}'') + (q\bar{q}' \to Wb\bar{b}q\bar{q}) + (q\bar{q}'' \to Wb\bar{b}q'\bar{q}'') + (q''\bar{q}'' \to Wb\bar{b}q\bar{q}') + (q\bar{q} \to Wb\bar{b}q\bar{q}') + (qq \to Wb\bar{b}qq') + (qq' \to Wb\bar{b}qq) \tag{8}$$

$$PROC = 5: \quad (qg \to Wb\bar{b}q'q''\bar{q}'') + (qg \to Wb\bar{b}q'q\bar{q}) + (qg \to Wb\bar{b}qq\bar{q}') \tag{9}$$

$$PROC = 6: \quad (gg \to Wb\bar{b}q\bar{q}'q''\bar{q}'') + (gg \to Wb\bar{b}q\bar{q}'q\bar{q}) \; . \tag{10}$$

We did not indicate possible additional final-state gluons, and did not explicitly list trivial permutations of the initial state partons and charge-conjugated processes. This list of processes fully covers all those possible in the case of up to 3 jets in addition to the b and $\bar{b}$. In the case of 4 extra jets, we did not include processes with 3 light-quark pairs. Within the uncertainties of the LO approximation, these can be safely neglected [2]. The matrix elements are obtained using ALPHA, which calculates the Green function generator via an exact numerical iterative algorithm, as explained in [11].

Note that PROC=6 only contributes to ≥ 4 light-jet production; PROC=5 only contributes to ≥ 3 light-jet production; PROC=3 and 4 only contribute to ≥ 2 light-jet production; PROC=2 only contributes to ≥ 1 light-jet production; PROC=1 contributes to all $Wb\bar{b} + X$ final states. Every time the jet multiplicity is increased, new classes of processes appear. These new processes cannot be simply obtained by adding one extra gluon to the lower-order ones. As a result, their rate cannot be estimated in a shower MC approach, where lower-order processes are allowed to evolve and emit more jets due to gluon radiation. This fact stresses once more the importance of a complete parton-level calculation of all relevant matrix elements.

In the cases where comparisons with existing results were possible, we verified that our code reproduces previous calculations. We carried out these tests at the level of total cross sections for the massive $Wb\bar{b}$ case (comparing with the results of [22]), and for $Wb\bar{b}$ plus up to 2 extra jets, for massless b (comparing with the results obtained running the VECBOS code[3]).

All calculations are performed using MC techniques, and the resulting code can be used as an event generator. For each generated event the code provides the full kinematics and flavours of the external partons, selected according to the relative probabilities, as well as the colour flow. The code includes an interface to HERWIG, allowing the events to be fully evolved through the coherent parton shower, and to be hadronized. The full code, as well as more detailed documentation, are available from the URL: `http://home.cern.ch/mlm/wbb/wbb.html`.

4 Study of the partonic results

In this section we present some numerical results for parton-level cross-sections and distributions, using experimental configurations corresponding to the upgraded Tevatron Collider ($p\bar{p}$ collisions at $\sqrt{s} = 2$ TeV) and to the LHC (pp collisions at $\sqrt{s} = 14$ TeV). As default parameters for our calculations we shall use: $m_W = 80.23$ GeV, $\Gamma_W = 2.03$ GeV, $m_b = 4.75$ GeV, PDF set CTEQ5M [25], with 2-loop $\alpha_s(Q^2)$, and renormalization/factorization scales $\mu_R^2 = \mu_F^2 = m_W^2 + \langle p_T^2 \rangle$, where $\langle p_T^2 \rangle$ is the average p_T^2 of all outgoing jets.

We shall define here as light jets those formed by the light quarks and gluons. They are required to be separated from each other, and from the b quarks, by $\Delta R_{ij} > 0.4$, with $\Delta R_{ij} = [(\eta_i - \eta_j)^2 + (\phi_i - \phi_j)^2]^{1/2}$ for each pair of partons i and j. The cut at $\Delta R_{ij} > 0.4$, rather than at the value of $\Delta R_{ij} > 0.7$ used as standard in jet physics at the Tevatron, is motivated by the choice of jet definition used in most top-quark studies at the Tevatron [26]. We shall analyse later the impact of this choice on the comparison between jet rates at the parton level and at the fully-showered level. Finally, all jets are also required to be hard and central:

$$p_t^i > 20 \text{ GeV}, \quad |\eta_i| < 2.5 \tag{11}$$

We shall not set any cut on the charged lepton and on the neutrino (giving rise to missing transverse energy, $\not{E}_T$) from the W decay, and we shall present rates including only one possible leptonic flavour in the W decay.

In the following, we shall use the symbol N_J to indicate the total number of jets, including the jets generated by the b or $\bar{b}$ quarks.

[3] `http://www-theory.fnal.gov/people/giele/vecbos.html`

Process	$N_J = 2$	$N_J = 3$	$N_J = 4$	$N_J = 5$	$N_J = 6$
1	360(1)	68.6(4)	10.4(1)	1.46(1)	0.20(1)
2	–	37.6(2)	12.1(1)	2.63(3)	0.47(1)
3+4	–	–	4.3(1)	1.66(3)	0.41(1)
5	–	–	–	0.085(2)	0.036(1)
6	–	–	–	–	0.00038(2)
Total	360(1)	106.4(4)	26.8(2)	5.84(4)	1.11(2)

Table 1: Contributions from different initial states to the $p\bar{p} \to (W \to \ell\nu)b\bar{b}j_3 \dots j_{N_J}$ rates (fb), for the Tevatron at $\sqrt{S} = 2$ TeV, with the cuts given in eq. (11). The different processes are defined in eqs. (5)-(10). The – indicates that the process is not available for the given jet multiplicity. The PDF set is CTEQ5M, and only one lepton flavour is considered. The uncertainties (quoted in parentheses as errors on the last significant figure) reflect the statistical accuracy of our MC evaluation.

Process	$N_J = 2$	$N_J = 3$	$N_J = 4$	$N_J = 5$	$N_J = 6$
1	2.60(1)	0.63(1)	0.144(3)	0.036(2)	0.008(1)
2	–	2.97(1)	2.11 (2)	1.08(2)	0.47(2)
3+4	–	–	0.288(1)	0.24(1)	0.13(2)
5	–	–	–	0.030(1)	0.031(4)
6	–	–	–	–	0.0010(3)
Total	2.60(1)	3.60(1)	2.54(2)	1.38(2)	0.64(3)

Table 2: Same as Table 1, for the LHC. Rates in pb.

4.1 Total rates

We start by considering final states where both b and $\bar{b}$ are sufficiently hard and well separated to form independent jets, and apply to them the same cuts defining light jets, namely $\Delta R_{b\bar{b}} > 0.4$ and eq. (11). We shall call these "2-b-jet events". Table 1 gives the rates for final states with 2 b jets plus extra light jets at the Tevatron, with the contributions from the different classes of processes listed separately. The Table shows that, for multiplicities up to 4 jets, the qualitatively new processes appearing every time the multiplicity is increased by one are of the same order, or larger, as the processes obtained from the lower-order channels by radiating one extra gluon.

The results for the LHC are given in Table 2. Note here that the effect of the new processes appearing for larger jet multiplicities is even more important. This is due to the fact that the lowest-order process involving initial state antiquarks is strongly suppressed by the sea-quark density relative to higher-order final states, which are enhanced by the large initial-state gluon contribution. This result is consistent with the numbers quoted in Table 7 of [2] in the case of massless b.

Since experimentally one does not always require the identification of both b and $\bar{b}$, it is important to consider, in addition to the case of 2-b-jet events, cases where the event has only one taggable b jet. These events receive contributions from final states where either one between the b and $\bar{b}$ is too soft or outside the rapidity range for the jet definition, or where the b and $\bar{b}$ are close enough as to merge into a single jet. If we treated the b as a massless particle, both these limiting cases would lead to infinite rates at LO, due to soft or collinear divergences. Only the inclusion of NLO virtual corrections, with an infrared and collinear safe jet definition, would restore a finite and physical answer. Since we treat the b quark as massive, the LO calculation is however meaningful and finite (expressing the fact that the "b-ness" of a jet is in principle measurable via its decays regardless of how small its energy is, and regardless of how collinear the b-$\bar{b}$ pair is).

We can therefore define and predict the rates for final states where only one jet is taggable. We call these "1-b-jet events". More specifically, 1-b-jet events are those which fail the 2-b-jet definition, but fall in one of these classes:

1. One between the b and the $\bar{b}$ satisfies eq. (11).
2. Both b and $\bar{b}$ fail eq. (11), but

$$\Delta R_{b\bar{b}} < 0.4,\ p_t(\vec{b}+\vec{\bar{b}}) > 20\ \text{GeV},\ |\eta(\vec{b}+\vec{\bar{b}})| < 2.5\ . \tag{12}$$

For these events, production of a $W + N_J$-jet final state requires an $\mathcal{O}(\alpha_s^{N_J+1})$ process, as one extra light-parton jet is needed to give the required jet multiplicity. In spite of the presence of the extra power of α_s, the contribution of these events to the 1-tag final states can be very large, because of the presence of potentially large soft and collinear logarithms. This is confirmed by Table 3, which shows that the contribution to single-tag events coming from the higher-order processes is as large as that of the leading-order ones[4]. In the case of the LHC, Table 4, the higher-order contributions are significantly larger than the leading-order ones, consistently with the results shown for the multiplicity-dependence of the total jet rates in Table 2. This is particularly true for the process most relevant to the study of associated WH production, where the $\mathcal{O}(\alpha_s^3)$ process is almost 5 times larger than the $\mathcal{O}(\alpha_s^2)$ one. The requirement of double-b tagging is very important in this case to efficiently reduce this extra background.

Before concluding this section we stress that all rates shown in the Tables are affected by a large overall uncertainty due to the choice of renormalization and factorization scales. Since the matrix-element calculations only include the LO contributions, and given the large powers of α_s which multiply the rates (the processes with N_J final state partons scale like $\alpha_s^{N_J}$), one should assume overall systematic uncertainties of the order of a factor of 2-4, depending on the jet multiplicity. In principle, this uncertainty can be reduced by using the information coming from data on $W + N_J$ jets (without final-state b jets) or $Z + +b\bar{b} + n$ jets, which are not affected by the contamination of the $t\bar{t}$ signal. The calculation of the $Z + b\bar{b} + n$ jet processes will be done in the future.

[4] The actual relative contribution of 2-b-jet events and 1-b-jet events to the single-tagged rate depends on the experimental value of the tagging efficiency, which will depend on the structure of the b jet. We expect, for example, that tagging efficiencies for semileptonic tags will be approximately a factor of two larger for jets containing two b than for single-b jets.

Perturbative Order	$N_J = 1$	$N_J = 2$	$N_J = 3$	$N_J = 4$	$N_J = 5$
$\mathcal{O}(\alpha_s^{N_J})$	–	360(1)	106.4(4)	26.8(2)	5.84(4)
$\mathcal{O}(\alpha_s^{N_J+1})$	1316(3)	371(2)	94.0(5)	20.5(4)	3.8(1)

Table 3: Contributions to $W + N_J$-jet rates (fb) at the Tevatron, from final states with 2 (upper row) or 1 (lower row) b-jets.

Perturbative Order	$N_J = 1$	$N_J = 2$	$N_J = 3$	$N_J = 4$	$N_J = 5$
$\mathcal{O}(\alpha_s^{N_J})$	–	2.60(1)	3.60(1)	2.54(2)	1.38(2)
$\mathcal{O}(\alpha_s^{N_J+1})$	9.38(5)	12.3(1)	7.4(1)	3.71(5)	1.7(1)

Table 4: Contributions to $W + N_J$-jet rates (fb) at the LHC, from final states with 2 (upper row) or 1 (lower row) b-jets.

4.2 Jet distributions

We present in this subsection some interesting distributions for parton-level multijet events. Figure 1 shows the inclusive p_T distribution of b jets, for final states with jet multiplicities N_J = 2-5. We compare the distributions of b jets in 2-b-jet and 1-b-jet events, where in the first case each event will contribute two entries to the histograms. The shapes of the two distributions are rather similar through most of the energy range. The curve relative to 2-b-jet events has a larger normalization because of the double probability of finding a b jet in the event.

The large contribution coming from events where only one b jet is reconstructed is clearly visible. To show the impact that such events have on the background to the associated production of a W boson and a resonance decaying to a b pair (e.g. a Higgs boson), we present in fig. 2 the invariant mass spectrum of the dijet pair in dijet events. The solid line corresponds to the $\mathcal{O}(\alpha_s^2)$ process, where both b quarks give rise to independent jets. The dashed line corresponds to the 1-b-jet events obtained from the $\mathcal{O}(\alpha_s^3)$ process. This figure shows that the requirement of having two independently b-tagged jets is crucial for the background suppression. A detailed study of the tagging efficiencies for 1-b-jet events is necessary to ensure that the residual contribution from fake tags on the second, non-b, jet is small.

To explore more in detail the structure of the b jet in 1-b-jet events, we plot in fig. 3 the ΔR separation between the b and the $\bar{b}$, showing the curves for different ranges of p_T of the b jet. Events where $\Delta R > 0.4$ correspond to cases where one of the two bs is either too soft or is outside the rapidity range. The figures show that at large p_T we are dominated by 1-b-jets with the b and $\bar{b}$ merged inside the jet ($\Delta R < 0.4$). The tagging efficiency for these jets is presumably larger than that for jets made of a single b, in particular if semileptonic tags are considered. It is an important experimental issue to evaluate what the actual tagging efficiency is for these jets, as a function of p_T.

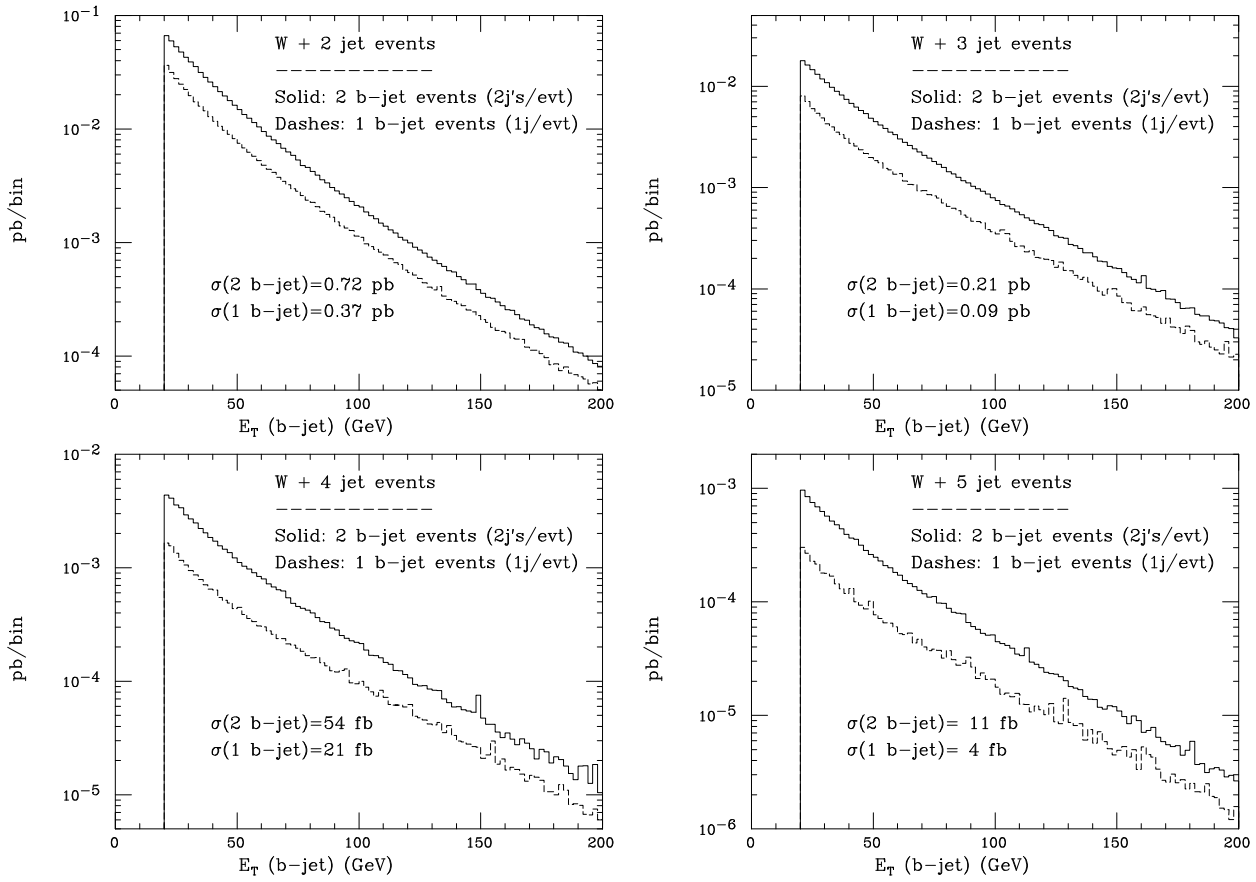

Figure 1: Inclusive p_T distributions of b jets. The solid lines refer to 2-b-jet events (in which case both jets are entered in the histograms); the dashed lines refer to 1-b-jet events.

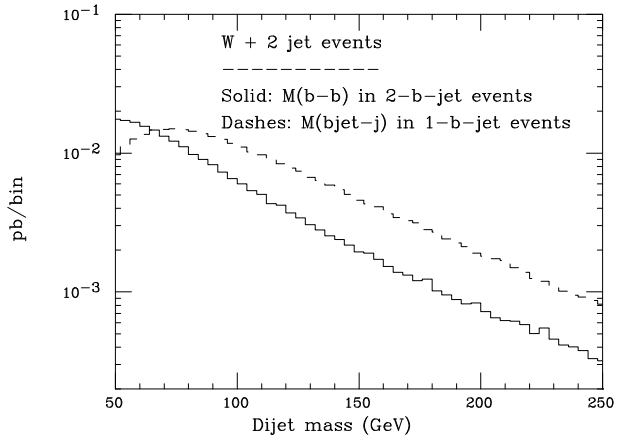

Figure 2: Dijet invariant mass distribution, in W plus 2 jet events, where at least one of the two jets has a b in it. The solid line refers to 2-b-jet events; the dashed line refers to 1-b-jet events.

5 Study of the fully showered final states

In this Section we describe the results obtained after evolution through the parton shower. The goal of our calculations is to be able to generate as accurately as possible the full jet structure of the partons generated at the matrix-element level. We first generate a sample of parton-level events with a fixed multiplicity (N_J), and then process these events through HERWIG for the shower evolution. When applied to an event with N_J hard final-state partons, we expect that the parton-shower evolution will generate an event with an N_J-jet inclusive final state. Initial or final state radiation may change the overall jet multiplicity (e.g. by splitting a jet in two, or radiating a new one from the initial state), but these effects are of order α_s relative to the inclusive N_J-jet properties of the event. In principle one could use the shower evolution to predict the rates for configurations with jet multiplicities larger than N_J [27, 28]. We shall give examples later on of how well the MC succeeds in this goal. As is well known, however, the shower MCs tend to underestimate the fraction of events with extra jets, unless explicit matrix-element corrections for the emission of hard and non-collinear radiation are included. Algorithms exist for implementing these matrix-element corrections in the case of low jet multiplicity processes (corrections to DY production [29], top decays [30], WZ-pair production [31]), but their extension to the case of high-jet multiplicities we are interested in is currently severely limited by the complexity of these processes.

In the following two subsections we present some tests of our scheme. In the first one we discuss some sanity checks of our approach, showing that the inclusive properties of N_J-jet final states are preserved by the shower evolution. In the second subsection we discuss the ability of the shower MC evolution to predict the emission rates for extra jets.

5.1 Sanity checks

To start with, we compare the inclusive jet rates before and after evolution. While the evolution of the partonic events through HERWIG can generate fully hadronized final states, we chose here to

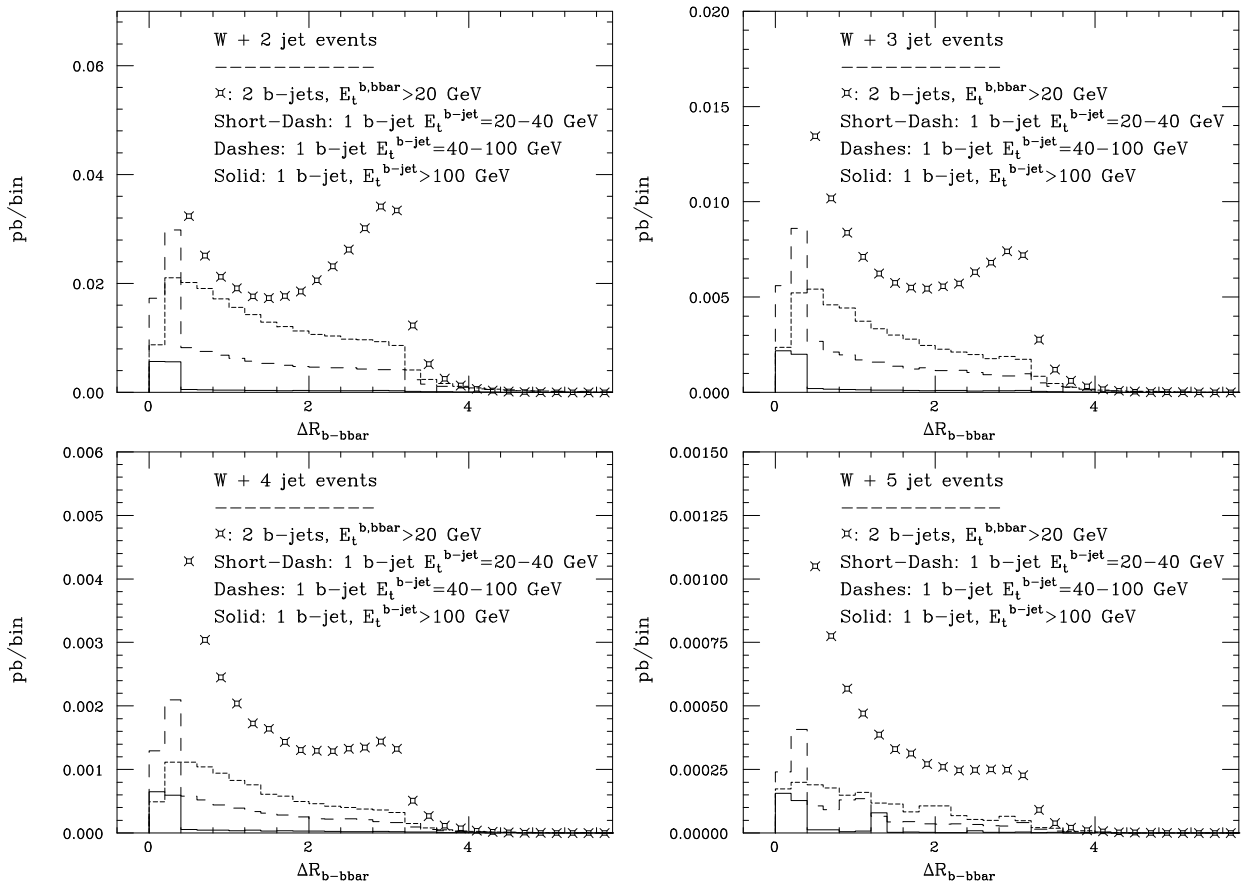

Figure 3: $b\bar{b}$ angular correlations in events with 2 b jets (plots) and with 1 b jet (histograms). The case of 1 b jet is divided into subsamples defined by the p_T of the b jet in the ranges 20-40, 40-100 and > 100 GeV.

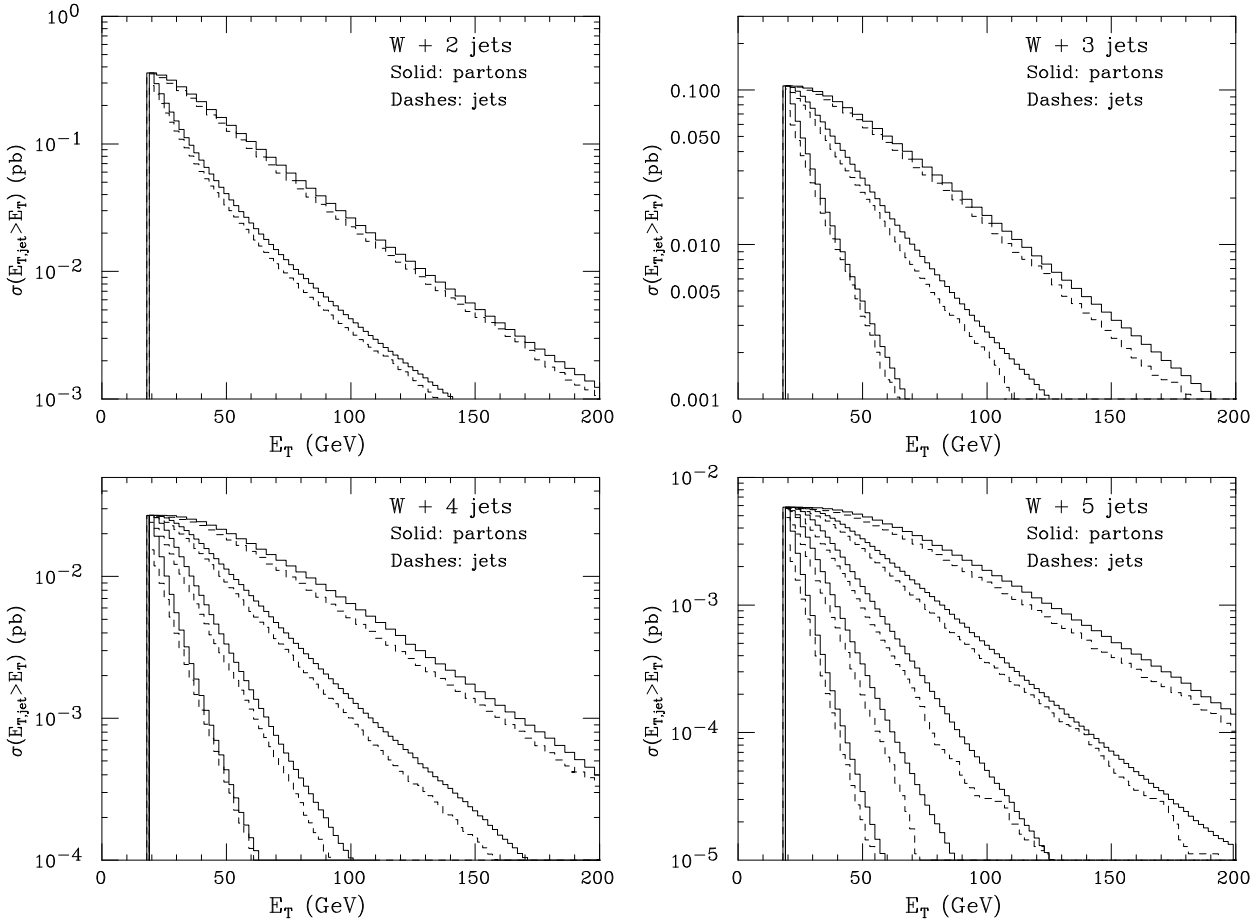

Figure 4: Inclusive p_T distributions of jets at the parton level (solid curves) and after shower evolution (dashed curves). The curves are ordered going from the hardest to the softest jet in the event. Parton level jets are defined by an isolation cut $\Delta R > 0.4$, and showered jets by a cone $R_{jet} = 0.4$.

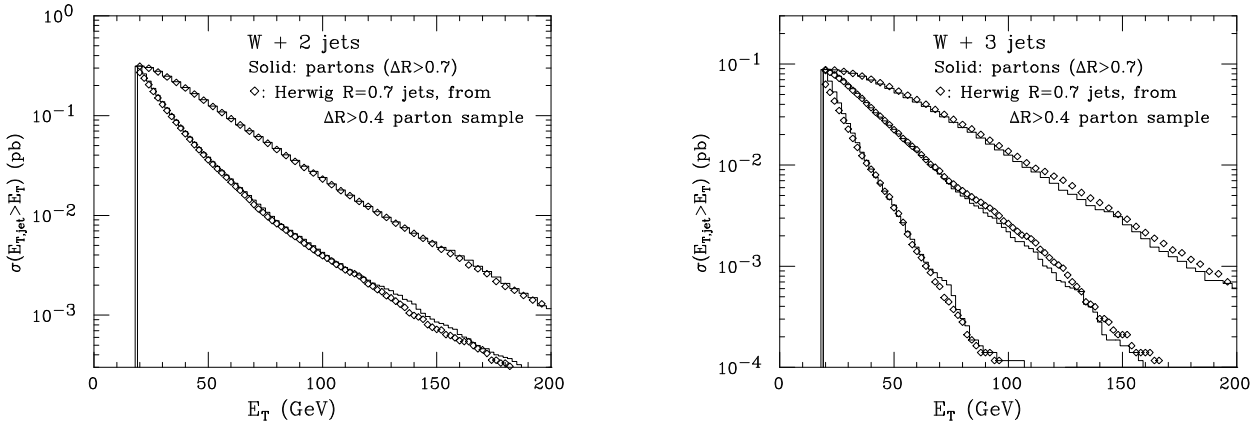

Figure 5: Inclusive p_T distributions of jets at the parton level, with separation cut $\Delta R > 0.7$ (solid curves), and of fully-showered $R_{jet} = 0.7$ jets (dashed curves). These last were obtained starting from the full sample of $\Delta R > 0.4$ partonic events.

stop the evolution after its perturbative part, in order to be able to compare as closely as possible the effects of higher-order perturbative corrections to the evolution of the final state. For the jet clustering after the shower evolution we use the standard cone algorithm, implemented in the routine GETJET [32] provided with the HERWIG code. To match the cuts used at the parton level, we use $R_{jet} = \Delta R = 0.4$, and a jet p_T threshold of 20 GeV.

Figure 4 compares the p_T spectra at parton level with those after the shower, for events generated at the parton level with 2, 3, 4 and 5 jets. The pair of curves correspond to the series of jets, from the hardest to the softest one. The curves show that the spectra after radiation do not exactly coincide with those at the parton level. The difference is consistent with an average energy-loss of 3-4 GeV outside the jet cone. One should therefore expect that a better matching of the partonic and fully showered jet spectra will be achieved by using wider jet cones, since these will more efficiently contain the energy radiated by the partons during their evolution. That this is the case, is shown in fig. 5. Here we compare the spectra obtained using a cut of $\Delta R > 0.7$ on the partons with those relative to fully showered jets defined by a cone of $R_{jet} = 0.7$. To generate this sample of $R_{jet} = 0.7$ jets we used the sample of parton-level events defined by the $\Delta R > 0.4$ cut, in order to cover the cases where two partons merge into a single jet, and extra jets are produced by the radiative processes. The agreement between the spectra is now perfect, consistently with the results obtained in the 2-jet case in [27]. The message here is that when preparing parton-level samples to be used for the QCD evolution by a shower MC algorithm, it is important to set generation cuts looser than those used in the definition of the full jets, in order to account for downward fluctuations in the jet energy and for jet merging induced by the jet clustering algorithms. In principle these problems should be avoided by using jet algorithms based on k_T clustering [33].

Figure 6 shows the matching between the directions of the partons before the shower, and the direction of the fully evolved jets. We note a smearing of the direction, which is more enhanced in the case of the soft jets, as should be expected. The matching of the jet momenta before and after the shower is shown in fig. 7. The distributions show on average a momentum loss, mostly due to radiation outside the jet cone, but have a width which is only of the order of 5-10% of the parton momentum.

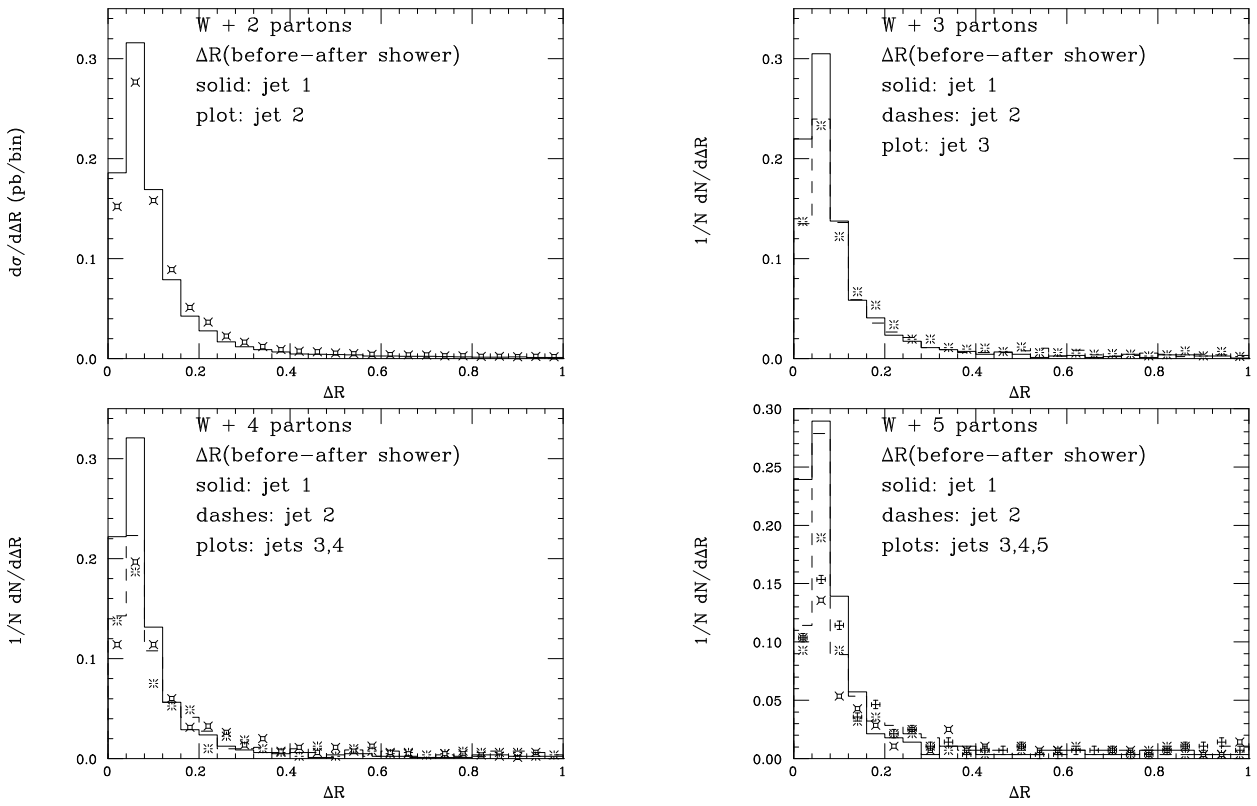

Figure 6: Parton-jet alignment. We plot the distance ΔR between the direction of the parton before radiation, and that of its daughter jet. Jets are labeled in decreasing order of p_T.

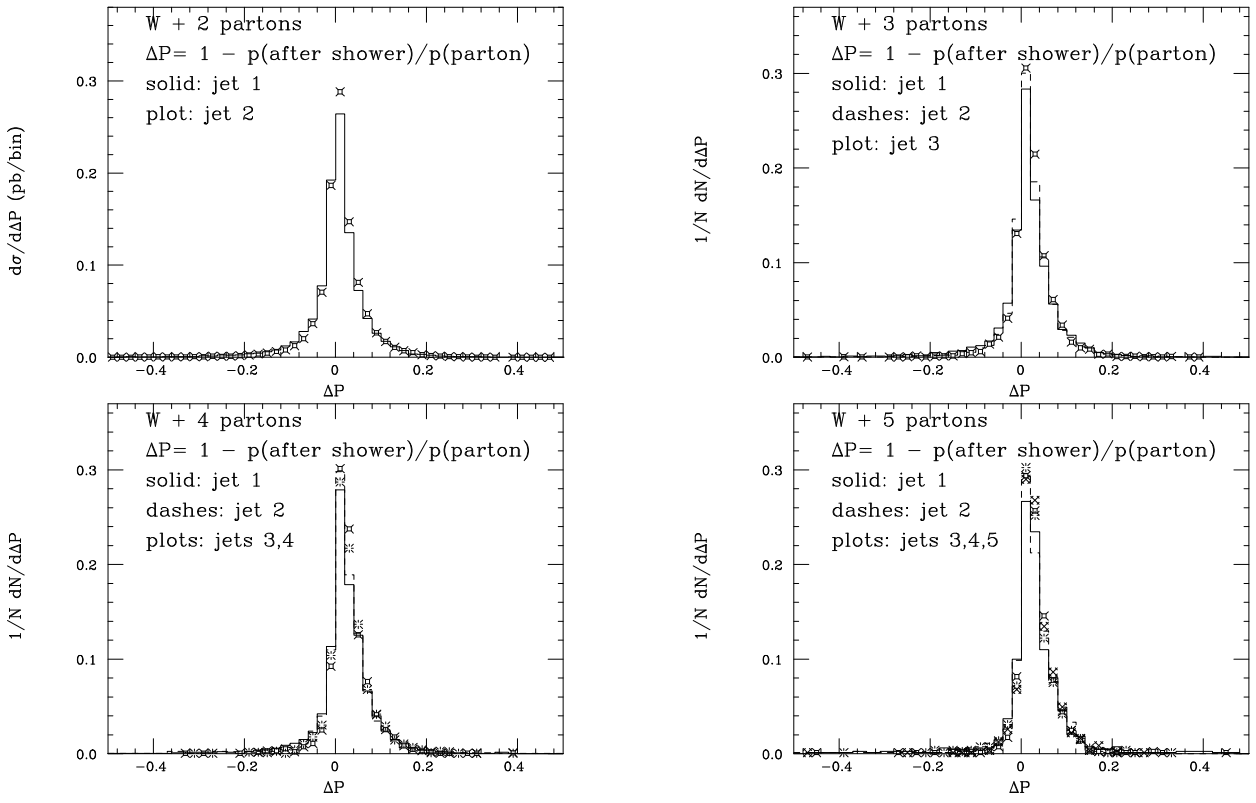

Figure 7: Jets' momentum matching. We plot the difference between the momentum of the parton before radiation and that of the jet, normalized to the parton momentum. Jets are labeled in decreasing order of p_T.

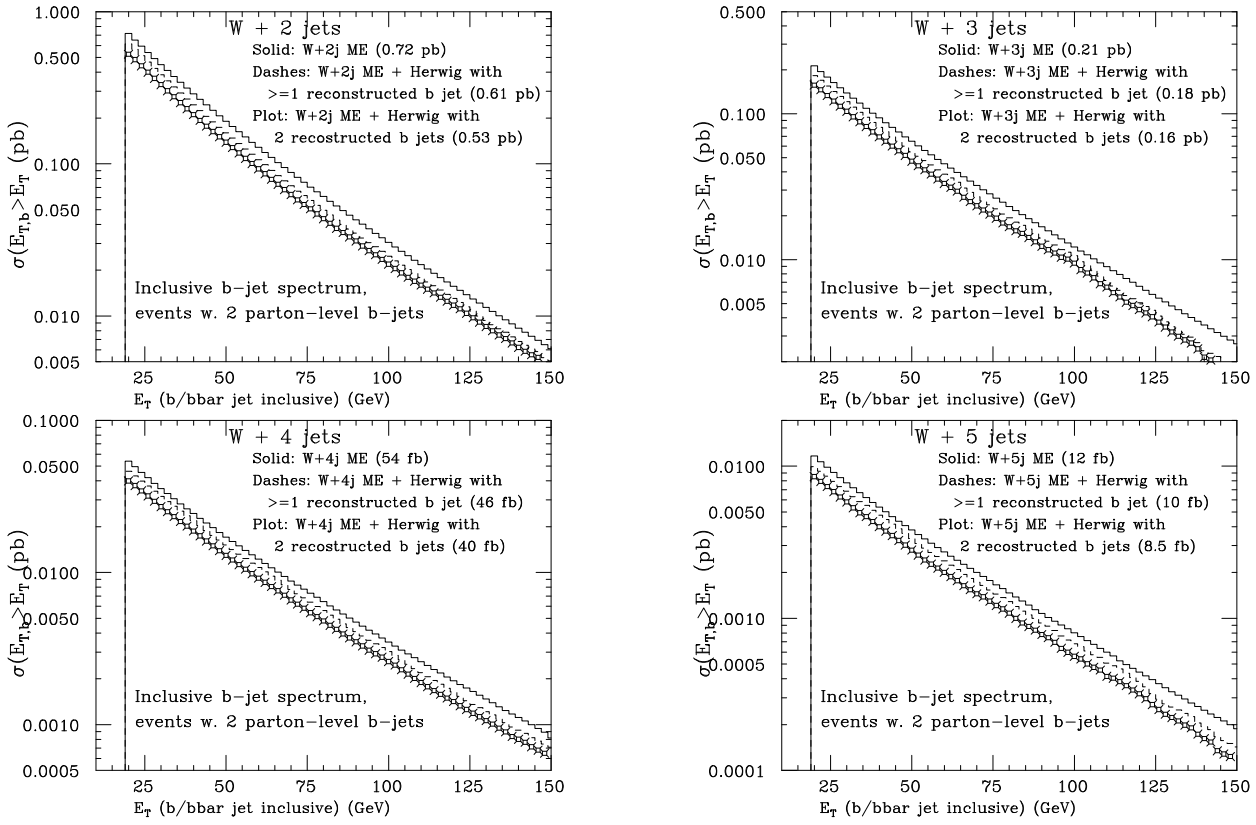

Figure 8: Inclusive spectrum of b jets: the result for 2-b-jet parton-level events (solid) is compared to the spectrum obtained for the same events after shower evolution (dashed line); the plotted points correspond to the result for events which have still 2 b jets after the shower evolution).

In fig. 8 we display the comparison between the inclusive spectra of b jets, before and after shower evolution. At the parton level we use events with 2-b-jets. Only a fraction of them will survive as 2-b-jet events after the shower, once again due to some energy loss outside the cone, and to artifacts of the jet merging during the clustering.

The outcome of all these studies is that the shower evolution preserves the inclusive properties of parton-level events, up to corrections induced by energy losses outside the small, $R_{jet} = 0.4$, jet cones.

5.2 Jet radiation in HERWIG

We address in this section the issue of the ability of the shower MC to correctly predict the rate for hard radiation leading to extra final-state jets. The plots in fig. 9 show the spectrum of the $(N_J + 1)$-th jet in events obtained by evolving through HERWIG parton-level events with N_J jets. These spectra are compared with what obtained by using directly the $(N_J + 1)$-jet parton-level matrix elements, before (solid lines) and after (dashed lines) the HERWIG evolution. As we pointed out in a previous section, large contributions arise when higher-order parton level processes

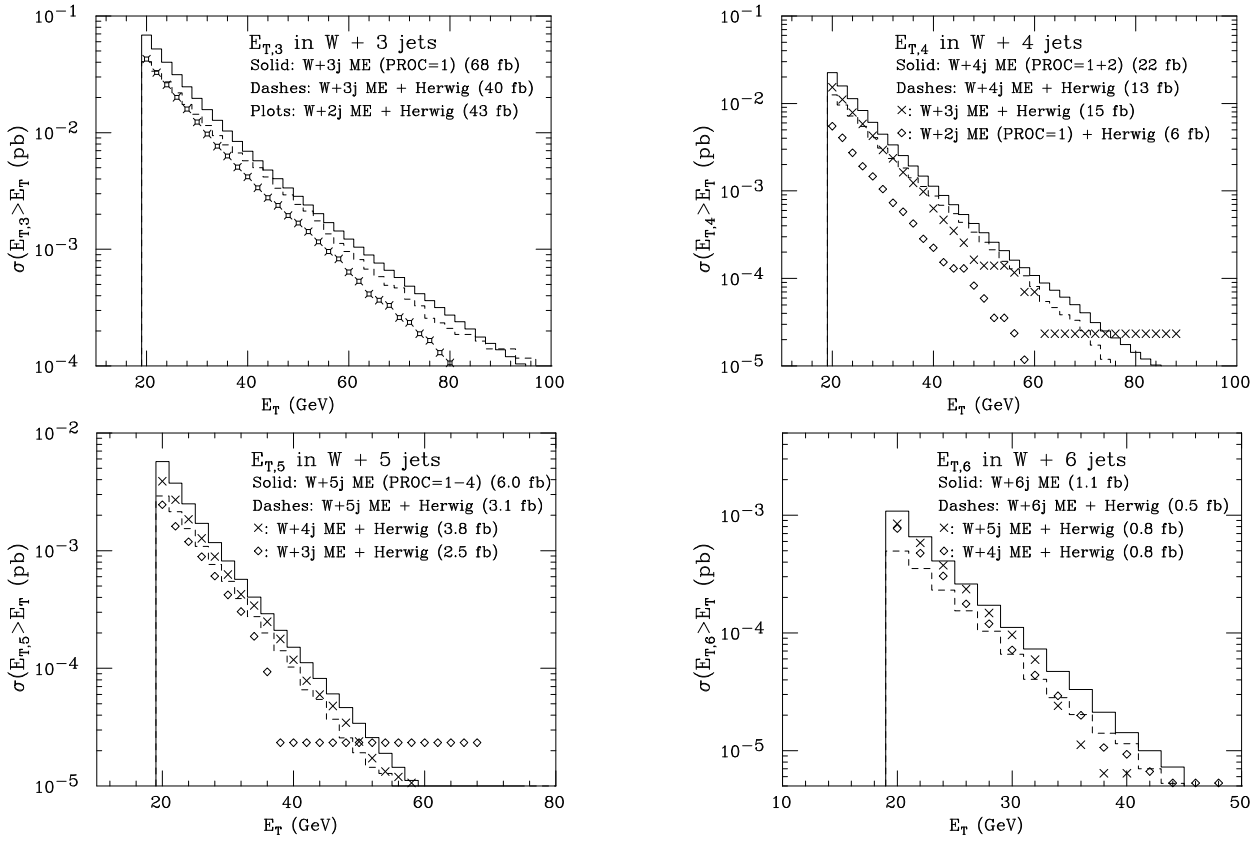

Figure 9: Comparison of jet rates evaluated with matrix elements with those obtained from hard radiation during the shower evolution of lower-order parton-level processes.

are considered. These contributions are due to the appearance of new processes, which cannot be generated via radiation processes in the MC (e.g. new initial states not present at the lower orders). In order to make a fair comparison, we therefore included in the parton-level estimate of the $(N_J + 1)$-th jet spectrum only those processes which are present at order $\alpha_s^{N_J}$. In the case of 3 final-state jets, we find a good agreement in the range $p_T \lesssim 45$ GeV between the rates obtained by evolving 3-jet parton level events through HERWIG (plotted points) and the rates obtained via radiation during the shower evolution of 2-jet parton-level events (dashed line). A similar result is obtained in the case of 4 jets. In this case we also studied the prediction of HERWIG based on 2-jet parton-level events, probing therefore the ability to predict the rate for the emission of 2 extra jets (diamond symbols). The deficit in 4 jets predicted using the 2-jet matrix elements is in part due to the lack of qg-initiated processes, which account for 35% of the 3-jet rate. Even including this correction, however, we see that not enough hard radiation is emitted to correctly predict the emission of 2 extra jets. The situation is improved when considering 5 and 6 jets, as shown in the last frames of fig. 9, presumably because the overall amount of energy present in the events in this case improves the validity of the soft-gluon emission approximation even in the case of radiation leading to emission of 2 extra jets.

6 Conclusions and outlook

In this work we presented a general framework for the evaluation of complex multiparton matrix elements, including an algorithm for the consistent merging with a coherent shower evolution, leading to fully hadronized multijet final states. We applied these ideas to the specific case of $Wb\bar{b}+n$ jet production, completing the calculation for processes with up to a total of 6 final-state partons (including the b and $\bar{b}$). We presented results both at the parton level, and after the shower evolution, which was done using the HERWIG MC. In addition to providing a proof of feasibility for these calculations and to showing the consistency of the merging with the coherent shower evolution, we pointed out several important consequences of the higher-order calculations and of the ability to maintain a non-zero mass for the b quarks. On one side we stressed the fact that jet rates do not obey the naive α_s scaling with multiplicity, due to the appearance at higher orders of new, large contributions. This is especially true in the case of the lowest-order $Wb\bar{b}$ and $Wb\bar{b}+j$ processes, and it is even more remarkable in the case of pp collisions at the LHC. On the other side, we pointed out that measurements done by requiring the presence of only one tagged b jet are very sensitive to the contribution of 1-b-jet events, namely events where the b jet contains both the b and the $\bar{b}$ quarks, or where one of the two b does not reconstruct a taggable jet. The impact of these events on the background subtraction needed to determine the top cross section from the current measurements performed at the Tevatron remains to be assessed.

The formalism we have outlined, and the key use of ALPHA to enable the calculation of the matrix elements and the extraction of the colour information needed for the coherent shower evolution, are readily portable to the study of other complex multiparton processes. The removal of the $b\bar{b}$ pair from the calculation will immediately lead to the evaluation of $W+n$ jet rates, with n up to 4. While these processes have already been studied in the literature, and have been encoded in the VECBOS MC, our approach will add to the existing tools the ability to consistently evolve the final states through the shower MCs, and to generate events suitable for realistic detector simulations. The work on the $W+n$ jet program is in progress. If one can neglect contributions from subprocesses with 6 or more light quarks, an extension to n up to 6 will be readily available using the ALPHA code. Inclusion of the processes with 6 or more light quarks presents no conceptual problems, but simply requires a more involved bookkeeping of all possible flavour channels.

The calculation of the processes $p^{(-)}p \to t\bar{t}b\bar{b}+n$ jets and $p^{(-)}p \to b\bar{b}b\bar{b}+n$ jets (with n up to 2) is being completed [5], and will soon be reported on. Future work will then include the study of $Zb\bar{b}+n$ jets and of $t\bar{t}+n$ jets.

Acknowledgements

MM and RP thank the CERN Theory Division for hospitality during various stages of this work.

References

[5] M.L. Mangano, G. Montagna, M. Moretti, O. Nicrosini, F. Piccinini and R. Pittau, work in progress.

[1] I. Hinchliffe, LBL-34372 *Submitted to Workshop on Physics at Current Accelerators and the Supercollider, Argonne, IL, 2-5 Jun 1993.*
[2] F. A. Berends, H. Kuijf, B. Tausk and W. T. Giele, Nucl. Phys. B **357** (1991) 32.
[3] F. A. Berends, W. T. Giele and H. Kuijf, Phys. Lett. B **232** (1989) 266.
[4] T. Stelzer and W. F. Long, Comput. Phys. Commun. **81** (1994) 357 [hep-ph/9401258].
[5] A. Pukhov *et al.*, hep-ph/9908288.
[6] T. Ishikawa, T. Kaneko, K. Kato, S. Kawabata, Y. Shimizu and H. Tanaka [MINAMI-TATEYA group Coll.], KEK-92-19.
[7] G. Marchesini and B. R. Webber, Nucl. Phys. B **310** (1988) 461. G. Marchesini, B. R. Webber, G. Abbiendi, I. G. Knowles, M. H. Seymour and L. Stanco, Comput. Phys. Commun. **67** (1992) 465. G. Corcella *et al.*, JHEP **0101** (2001) 010 [hep-ph/0011363].
[8] T. Sjostrand, Comput. Phys. Commun. **82** (1994) 74. T. Sjostrand, P. Eden, C. Friberg, L. Lonnblad, G. Miu, S. Mrenna and E. Norrbin, Comput. Phys. Commun. **135** (2001) 238 [hep-ph/0010017].
[9] F. E. Paige, S. D. Protopopescu, H. Baer and X. Tata, hep-ph/9810440.
[10] F. Caravaglios, M. L. Mangano, M. Moretti and R. Pittau, Nucl. Phys. B **539** (1999) 215 [hep-ph/9807570].
[11] F. Caravaglios and M. Moretti, Phys. Lett. B **358** (1995) 332 [hep-ph/9507237].
[12] P. Draggiotis, R. H. Kleiss and C. G. Papadopoulos, Phys. Lett. B **439** (1998) 157 [hep-ph/9807207].
[13] A. S. Belyaev *et al.*, hep-ph/0101232.
[14] K. Sato, S. Tsuno, J. Fujimoto, T. Ishikawa, Y. Kurihara and S. Odaka, hep-ph/0104237.
[15] A. Bassetto, M. Ciafaloni and G. Marchesini, Phys. Rept. **100** (1983) 201. L. V. Gribov, E. M. Levin and M. G. Ryskin, Phys. Rept. **100** (1983) 1.
[16] F. Abe *et al.* [CDF Coll.], Phys. Rev. D **50** (1994) 5562. B. Abbott *et al.* [D0 Coll.], Phys. Lett. B **464** (1999) 145 [hep-ex/9908017]. B. Abbott *et al.* [D0 Coll.], Phys. Lett. B **414** (1997) 419 [hep-ex/9706012].
[17] F. A. Berends and W. Giele, Nucl. Phys. B **294** (1987) 700. M. Mangano, S. Parke and Z. Xu, Nucl. Phys. B **298** (1988) 653.
[18] M. Mangano and S. J. Parke, Nucl. Phys. B **299** (1988) 673. F. A. Berends and W. T. Giele, Nucl. Phys. B **306** (1988) 759.
[19] M. L. Mangano and S. J. Parke, Phys. Rept. **200** (1991) 301.
[20] K. Odagiri, JHEP **9810** (1998) 006 [hep-ph/9806531].
[21] P. D. Draggiotis, A. van Hameren and R. Kleiss, Phys. Lett. B **483** (2000) 124 [hep-ph/0004047]. A. van Hameren and R. Kleiss, Eur. Phys. J. C **17**, 611 (2000) [hep-ph/0008068].
[22] Z. Kunszt, Nucl. Phys. B **247** (1984) 339. M. L. Mangano, Nucl. Phys. B **405** (1993) 536.
[23] R. K. Ellis and S. Veseli, Phys. Rev. D **60** (1999) 011501 [hep-ph/9810489].
[24] A. S. Belyaev, E. E. Boos and L. V. Dudko, Phys. Rev. D **59** (1999) 075001 [hep-ph/9806332].
[25] H. L. Lai *et al.* [CTEQ Coll.], Eur. Phys. J. C **12** (2000) 375 [hep-ph/9903282].
[26] F. Abe *et al.* [CDF Coll.], Phys. Rev. D **50** (1994) 2966. F. Abe *et al.* [CDF Coll.], Phys. Rev. Lett. **74** (1995) 2626 [hep-ex/9503002]. S. Abachi *et al.* [D0 Coll.], Phys. Rev. Lett. **74** (1995) 2632 [hep-ex/9503003].
[27] W. T. Giele, T. Matsuura, M. H. Seymour and B. R. Webber, FERMILAB-CONF-90-228-T *Contribution to Proc. of 1990 Summer Study on High Energy Physics: Research Directions for the Decade, Snowmass, CO, Jun 25 - Jul 13, 1990.* Published in Snowmass Summer Study 1990:0137-147.

[28] J.M. Benlloch, A. Caner, M.L. Mangano and T. Rodrigo, CDF/DOC/MONTECARLO/1823, Oct.1992. J. M. Benlloch [CDF Coll.], Published in the Proceedings of DPF 92, vol. 2, 1091-1093.
[29] M. H. Seymour, Comput. Phys. Commun. **90** (1995) 95 [hep-ph/9410414]. G. Corcella and M. H. Seymour, Nucl. Phys. B **565** (2000) 227 [hep-ph/9908388]. G. Miu and T. Sjostrand, Phys. Lett. B **449** (1999) 313 [hep-ph/9812455].
[30] G. Corcella and M. H. Seymour, Phys. Lett. B **442** (1998) 417 [hep-ph/9809451]. G. Corcella, M. L. Mangano and M. H. Seymour, JHEP **0007** (2000) 004 [hep-ph/0004179].
[31] M. Dobbs, hep-ph/0103174.
[32] GETJET, F. Paige and M. Seymour, private communication.
[33] S. Catani, Y. L. Dokshitzer and B. R. Webber, Phys. Lett. B **285** (1992) 291. S. D. Ellis and D. E. Soper, Phys. Rev. D **48** (1993) 3160 [hep-ph/9305266]. M. H. Seymour, Nucl. Phys. B **513** (1998) 269 [hep-ph/9707338].
[34] F. Abe *et al.* [CDF Coll.], Phys. Rev. Lett. **70** (1993) 4042.
[35] F. Abe *et al.* [CDF Coll.], Phys. Rev. Lett. **77** (1996) 448 [hep-ex/9603003].